American Mineralogist, Volume 88, pages 410–423, 2003

Si-Al disorder and solid solutions in analcime, chabazite, and wairakite

PHILIP S. NEUHOFF,[1,2,*] JONATHAN F. STEBBINS,[2] AND DENNIS K. BIRD[2]

[1]Department of Geological Sciences, University of Florida, Gainesville, Florida 32611-2120, U.S.A.
[2]Department of Geological and Environmental Sciences, Stanford University,
Stanford, California 94305-2115, U.S.A.

ABSTRACT

Quantitative determination of the abundance of Si(nAl) tetrahedral structural units (where n = 0, 1, 2, 3, or 4) through analysis of ^{29}Si magic angle spinning nuclear magnetic resonance (MAS NMR) spectra was used to assess the state of Si-Al disorder in the zeolites analcime [$(NaAl)_xSi_{48-x}O_{96}\cdot 16H_2O$], chabazite [$(Ca_{0.5},Na,K)_xAl_xSi_{12-x}O_{24}\cdot 12H_2O$], and wairakite [$CaAl_2Si_4O_{12}\cdot 2H_2O$]. Short-range Si-Al ordering in chabazite and analcime is a regular function of Al mol fraction and is fully consistent with Al avoidance, as has generally been reported for zeolites not subjected to heat treatment. The results of this study and previously reported ^{29}Si MAS NMR spectra suggest that natural analcime samples are more Si-Al ordered than either their synthetic counterparts or chabazite. Cluster variation method (CVM) calculations were used to calculate the configurational entropy (S_{CON}) due to Si-Al disorder in chabazite and analcime. The calculations predict that long-range Si-Al ordering develops when Al occupies 5 out of 12 tetrahedral sites in chabazite and synthetic analcime and 17 out of every 48 tetrahedral sites in natural analcime. The difference between the calculated entropies and ideal entropies of mixing was used to derive activity-composition relationships for Si-Al substitution in these frameworks. Comparison between calculated values of S_{CON} and the results of calorimetric and phase equilibrium studies on analcime indicate that the CVM accurately assesses S_{CON}. The ^{29}Si MAS NMR spectrum obtained for natural wairakite indicates that this mineral is largely Si-Al ordered, but comparison with a previously published spectrum indicates that natural and synthetic wairakites can exhibit significant variation in Si-Al disorder.

INTRODUCTION

Zeolites often exhibit complex compositional variations and substantial substitutional order-disorder. The energetic consequences of solid solution and disorder can often have a large effect on phase relations involving these minerals, especially given the relatively small changes in thermodynamic properties of reactions that govern zeolite stability (Chipera and Apps 2001; Neuhoff 2000; Neuhoff et al. 2000). With the growing interest in the use of natural zeolites in industrial processes and radioactive waste disposal (e.g., Colella et al. 2001; Kallo 2001; Ming and Allen 2001; Tchernev 2001), considerable effort has focused on understanding the thermodynamic properties of these minerals. This has led to numerous calorimetric and phase equilibrium studies of zeolites (e.g., Johnson et al. 1982, 1983; Kiseleva et al. 1996; Liou 1971a, 1971b, 1971c; Murphy et al. 1996). Despite these efforts, little information exists concerning the thermodynamic consequences of solid solution and disorder in zeolites, particularly with respect to Si-Al substitution in zeolite frameworks.

Neuhoff and Stebbins (2001) recently developed an athermal solid solution model describing the energetic consequences of Si-Al substitution in the frameworks of highly symmetrical zeolites (i.e., those whose crystal structure contains only one crystallographically distinct tetrahedral site). This model (recapitulated below) was based on calorimetric observations of negligible excess enthalpies of mixing for Si-Al substitution in zeolites (Petrovic and Navrotsky 1997; Shim et al. 1999) and negative excess entropies of mixing based on the compositional dependence of configurational entropies (S_{CON}) calculated from ^{29}Si magic angle spinning nuclear magnetic resonance (MAS NMR) observations (cf. Phillips and Kirkpatrick 1994). In zeolites with only one tetrahedral site, up to five peaks can be present in the ^{29}Si MAS NMR spectrum, corresponding to four-coordinated Si with 4 Al, 3 Al + 1 Si, 2Al + 2 Si, 1 Al + 3 Si, and 4 Si second nearest neighbors. These peaks are hereafter referred to as Si(nAl) pentads, where n is the number of Al atoms in the second nearest neighbor coordination shell. If Al avoidance is perfectly obeyed (i.e., there are no Al-O-Al linkages in the framework), then the relative intensities of peaks in the ^{29}Si MAS NMR spectrum exactly constrain both the framework composition and the distribution of Si-Al clusters in the framework up to the size of the pentads. Neuhoff and Stebbins (2001) applied this model to synthetic zeolites of the FAU and LTA structure types (cf. Meier et al. 2001) for which copious ^{29}Si MAS NMR spectra have been published. The veracity of this model for describing the energetic consequences of Si-Al substitution in these zeolites could not be tested because suitable experimental observations of equilibria involving these phases have not been conducted.

Equilibria involving natural zeolites have received considerably more attention and potentially provide a means of test-

* E-mail: neuhoff@ufl.edu

0003-004X/03/0203–410$05.00

Brought to you by | New York University Bobst Library Technical Services
Authenticated
Download Date | 1/21/16 12:53 PM

ing the models of Neuhoff and Stebbins (2001) and Phillips and Kirkpatrick (1994). Two rock-forming zeolites, analcime and chabazite (ANA and CHA structure types, respectively; Meier et al. 2001), exhibit tetrahedral frameworks that are characterized by a single tetrahedral site and thus potentially provide a means of testing these models. Analcime, in particular, has been the subject of numerous equilibrium studies (e.g., Liou 1971a; Murphy et al. 1996; Redkin and Hemley 2000; Thompson 1971; Wilkin and Barnes 1998). However, relatively few ^{29}Si MAS NMR studies have been performed on these materials. Consequently, results are reported here for new ^{29}Si MAS NMR spectra on analcime and chabazite, which along with previously published results, are used to derive activity-composition relationships for Si-Al substitution in these minerals. Published experimental and geologic observations of equilibria between analcime and albite are then used to assess the validity of S_{CON} derived from ^{29}Si MAS NMR spectra for analcime. In addition, a new ^{29}Si MAS NMR spectrum is presented for wairakite, which shares the ANA framework topology with analcime.

MATERIALS AND METHODS

Samples and characterization

The samples investigated in this study (Tables 1 and 2) were all hand-picked separates of natural minerals that were subsequently ground in an agate mortar (with the exception of ANA004, which was obtained in a powdered form). Sample identification and purity were confirmed through X-ray powder diffraction (XRPD) using a Rigaku θ-θ diffractometer with Cu$K\alpha$ radiation operating at 35 kV and 15 mA. No anomalous or previously unreported behavior was observed in the XRPD patterns for the samples studied. The compositions of minerals used in this study were determined by electron probe microanalysis (EPMA) with an automated JEOL 733A electron microprobe operated at 15 kV accelerating potential and 15 nA beam current using natural samples for calibration. Beam width was varied between 10 and 30 μm depending on grain size and raw counts were collected for 20 s and converted to oxide weight percents using the CITZAF correction procedure after accounting for unanalyzed O atoms following the methods of Tingle et al. (1996).

The ANA framework samples used in this study are all phase pure natural samples. Sample ANA001 (the same analcime sample as that studied by Zhao et al. 2001) was purchased from Ward's Scientific and consisted of a several 0.5 to 8 mm grains of glassy to slightly opaque analcime from the Mt. St. Hilaire alkaline intrusive complex in Quebec, Canada. ANA002 was collected by the first author from a zeolite-facies metabasalt outcrop at Manillat on the island of Qeqetarssuaq in West Greenland and prepared from a 1.5 cm euhedral crystal of opaque analcime. The third analcime sample, ANA003, was donated by S. Kleine of Great Basin Minerals and was separated from a small sample of hydrothermally altered basalt (that also contained natrolite) from the Junnila benitoite claim in San Benito County, California. Sample ANA004 is a natural wairakite sample from the Onikobe geothermal system (see Seki et al. 1969 for details about this sample) that was donated by J.-G. Liou from stock remaining from his previous phase equilibrium studies on this mineral (Liou 1970, 1971b).

All of the chabazite samples used in this study are also phase pure. Sample CHA001was collected by the first author on the Gronau West Nunatak in East Greenland from a zeolite facies metabasalt and consisted of 2 to 3 mm sized pseudocubic crystals of slightly opaque chabazite. CHA002 was purchased from Mineralogical Research Company as a set of small samples of zeolite facies metabasalt containing subhedral glassy chabazite and gonnardite (same sample as the pure chabazite described by Neuhoff et al. 2002). Samples CHA003 and CHA004 were collected by the first author from different outcrops of zeolite-facies metabasalt near Breiddalsheidi, eastern Iceland. CHA003 was prepared from 1 to 2 cm penetration twins of pseudocubic chabazite that had weathered into the colluvium. CHA004 occurred as vesicle fillings along with thomsonite as 1 to 2 mm pseudocubic glassy crystals.

TABLE 1. Sample provenance and compositions for ANA structure zeolites

Sample	ANA001*	ANA002†	ANA003‡	ANA004§
Mineral	analcime	analcime	analcime	wairakite
Locality	Mont St. Hilaire, Canada	Manillat, West Greenland	San Benito Co., California	Onikobe, Japan
Si	32.25	32.83	32.05	4.02
Al	15.73	15.14	16.01	1.97
Ca	0	0	0	0.94
Na	15.84	15.25	15.84	0.08
Cs	0	0	0	0
K	0	0	0.24	0
Li	0	0	0	0
Rb	0	0	0	0
O	96	96	96	12
$Si/Al_{(analyzed)}$	2.06	2.15	2.02	2.04
$Si/Al_{(NMR)}$	1.95	2.10	1.86	–

* Purchased from Ward's Scientific.
† Geological Survey of Denmark and Greenland sample number 413386.
‡ Donated by S. Kleine, Great Basin Minerals.
§ Donated by J.-G. Liou.

TABLE 2. Sample provenance and compositions for CHA structure zeolites

Sample*	CHA001†	CHA002‡	CHA003	CHA004
Mineral	Chabazite	Chabazite	Chabazite	Chabazite
Locality	Gronau West Nunatak, East Greenland	Antrim County, Ireland	Breiddalsheidi, Iceland	Breiddalsheidi, Iceland
Si	8.15	7.66	7.74	8.25
Al	3.91	4.35	4.22	3.72
Ca	1.78	0.98	1.98	1.47
Na	0.04	0.38	0.23	0.75
K	0.07	1.17	0.13	0.16
Sr	0.00	0.35	0.03	0
O	24	24	24	24
$Si/Al_{(analyzed)}$	2.08	1.76	1.83	2.22
$Si/Al_{(NMR)}$	2.14	1.84	2.17	2.37

* Samples from first author's research collection unless otherwise noted.
† Geological Survey of Denmark and Greenland sample number 421552.
‡ Purchased from Mineralogical Research Co, San Jose, California.

Brought to you by | New York University Bobst Library Technical Services
Authenticated
Download Date | 1/21/16 12:53 PM

NMR spectroscopy

The ^{29}Si MAS NMR spectra were collected on a modified Varian VXR/Unity-400S spectrometer with a 9.4 Tesla (T) magnet (79.46 MHz for ^{29}Si). Approximately 300 mg of each sample were packed into 7 mm rotors and spun at 4.7 kHz. Spectra (consisting of 1000 to 10000 transients) were collected using a single 2 μs pulse (radio frequency tip angle of ~30°) using a relaxation delay of 10 s. This latter value was chosen to maximize signal to noise in the spectrum. Test spectra collected using longer relaxation delays exhibited identical relative peak intensities, indicating that differential relaxation between the signals was minimal. Spectra and chemical shifts (δ) were referenced to external tetramethyl silane. Peaks in ^{29}Si MAS NMR spectra were fit by least squares regression using the Varian VNMR software package. Errors in the fits are assumed to be on the order of 1% based on repeated fitting of the spectra using different starting values and peak shape models.

RESULTS

Analcime

Figure 1 shows the ^{29}Si MAS NMR spectra for analcime samples ANA001, ANA002, and ANA003 along with the fitting results listed in Table 3. Repeated attempts at fitting these spectra indicated that a pure Gaussian peak shape best described the observed resonances model and the spectra were fit accordingly. As can be seen in Figure 1 and Table 3, five sites were observed in ANA001, which were assigned to Si with zero to four Al next nearest neighbors based on the respective δ values and the approximately 5 ppm separation between the peaks (Engelhardt and Michel 1987; Phillips and Kirkpatrick 1994). The spectra for samples ANA002 and ANA003 did not exhibit signals from Si(4Al) and Si(0Al) pentads, respectively. Relative intensities of the various signals observed in the analcime samples change systematically with Si/Al ratio, in accordance with previous observations (Phillips and Kirkpatrick 1994). Comparison between the Si/Al ratios determined by EPMA and those calculated from the NMR spectra using the equation

$$\mathrm{Si}/\mathrm{Al} = \frac{4}{\sum_{n=1}^{4} n \bullet I_{\mathrm{Si}(n\mathrm{Al})}} \quad (1)$$

TABLE 3. ^{29}Si NMR data for analcime

Sample	Site	δ (ppm)	I*
ANA001	Si(4Al)	–86.4	0.011
	Si(3Al)	–91.0	0.195
	Si(2Al)	–96.2	0.637
	Si(1Al)	–101.0	0.145
	Si(0Al)	–106.0	0.111
ANA002	Si(3Al)	–91.4	0.164
	Si(2Al)	–96.5	0.594
	Si(1Al)	–101.6	0.222
	Si(0Al)	–107.0	0.020
ANA003	Si(4Al)	–86.9	0.020
	Si(3Al)	–91.2	0.227
	Si(2Al)	–96.4	0.642
	Si(1Al)	–101.3	0.111

* Relative intensity (peak area).

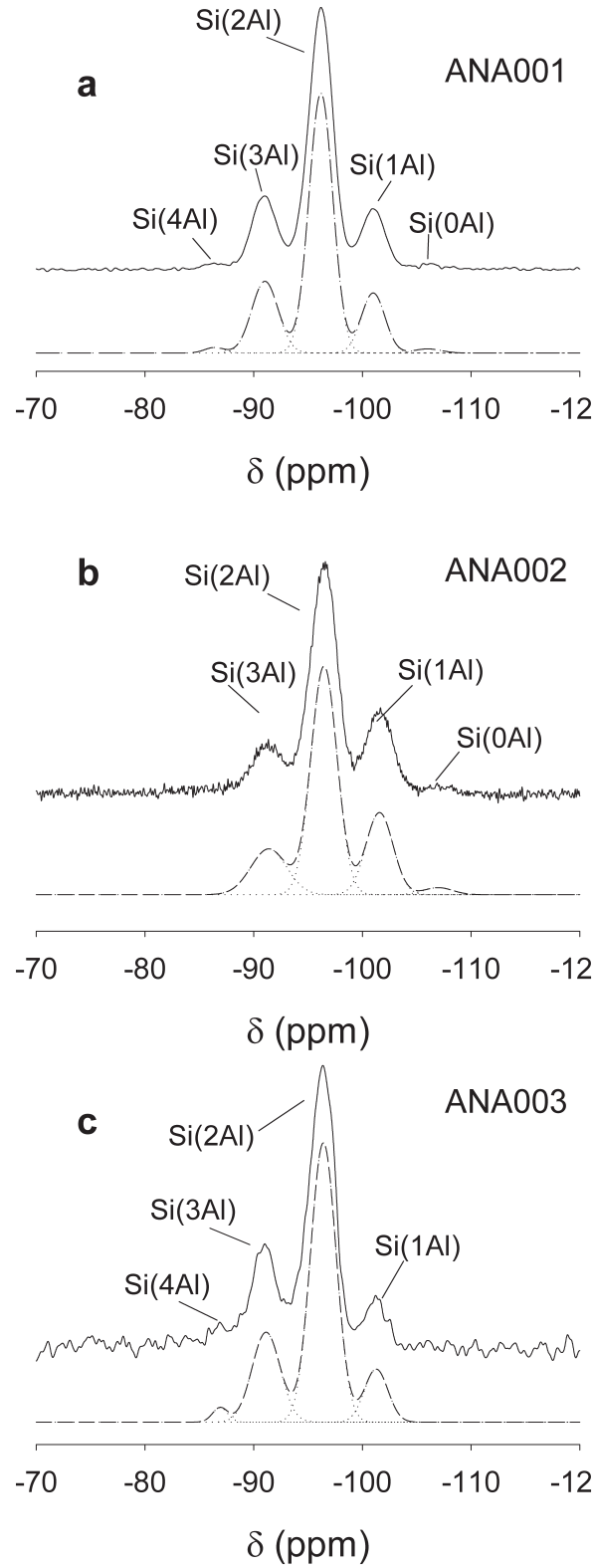

FIGURE 1. ^{29}Si MAS NMR spectra at 9.4 T for analcime samples ANA001 (**a**), ANA002 (**b**), and ANA003 (**c**). In each case, the upper spectrum is the experimental result and the lower corresponds to the fits listed in Table 3.

Brought to you by | New York University Bobst Library Technical Services
Authenticated
Download Date | 1/21/16 12:53 PM

where $I_{Si(nAl)}$ is the observed relative intensity of the Si(nAl) line in the ^{29}Si MAS NMR spectrum (Klinowski et al. 1982) indicate generally good agreement (corresponding to variations in the mole fraction of aluminum in the framework, X_{Al}, of less than 0.02) between the two methods (Table 1), suggesting that Al avoidance holds in these samples. Note also that the framework compositions determined by EPMA are slightly more Si-rich than those calculated from Equation 1; the reverse relationship would be expected if Al-O-Al linkages were present. The δ values listed in Table 3 for all three samples are consistent with those reported previously for analcime (e.g., Joshi et al. 1991; Kohn et al. 1995; Lippmaa et al. 1981; Murdoch et al. 1988; Nagy et al. 1985; Phillips and Kirkpatrick 1994). No resolution of signals arising from ^{29}Si on crystallographically distinct sites is observed in the spectra of Figure 1, despite evidence from crystal structure determinations that the true symmetry of analcime results in two to three distinct tetrahedral sites (Mazzi and Galli 1978). As noted by Murdoch et al. (1988), this likely reflects the very similar T-O-T bond angles among tetrahedral sites in analcime.

Chabazite

Figure 2 shows ^{29}Si MAS NMR spectra for chabazite samples CHA001, CHA002, CHA003, and CHA004 along with the fitting results listed in Table 4. As observed above for analcime and in previous studies of chabazite (e.g., Akporiaye et al. 1996; Bodart et al. 1988; Nagy et al. 1985; Thrush and Kuznicki 1991), five signals are present representing tetrahedral Si surrounded by zero to four Al next nearest neighbors. This is consistent with published structures of chabazite (Mazzi and Galli 1983), which suggest that only one crystallographically distinct site is present. The spectra were adequately described by these five signals assuming pure Gaussian lineshapes. In the case of CHA002, a small shoulder is present on the Si(4Al) peak toward the deshielded side which may indicate some sample heterogeneity (i.e., more than one chabazite phase with different T-O-T angles resulting in multiple peaks). Chemical shift values refined for the chabazite samples (Table 4) are consistent with those observed previously (e.g., Akporiaye et al. 1996; Bodart et al. 1988; Joshi et al. 1991; Lippmaa et al. 1981; Nagy et al. 1985; Takaishi and Kato 1995; Thrush and Kuznicki 1991). Aside from sample CHA003, Si/Al ratios determined by EPMA and Equation 1 are generally in good agreement (Table 2). The source of the discrepancy in the Si/Al values determined for CHA003 is unclear, but may in part be due to the fact that the Si/Al ratio determined from Equation 1 is an average (bulk) value, whereas the EPMA analysis listed in Table 2 is the average of several spot analyses. This conclusion is supported by the fact that our (unpublished) analyses of chabazite samples from the same outcrop as CHA003 span the

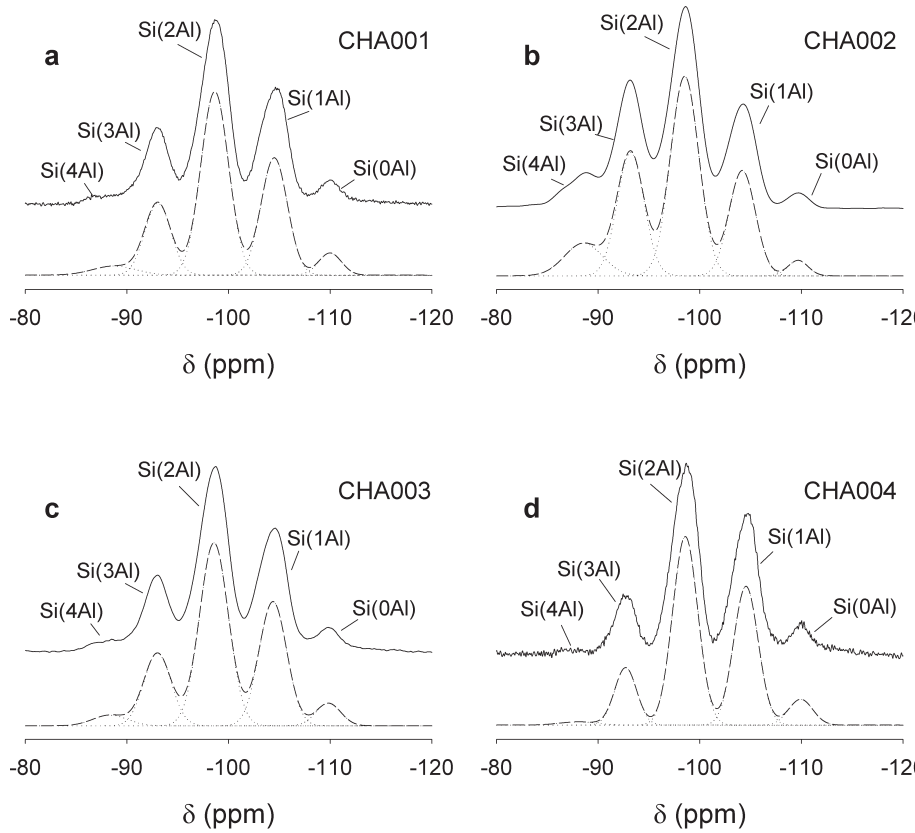

FIGURE 2. ^{29}Si MAS NMR spectra at 9.4 T for chabazite samples CHA001 (**a**), CHA002 (**b**), CHA003 (**c**) and CHA004 (**d**). In each case, the upper spectrum is the experimental result and the lower corresponds to the fits listed in Table 4.

Brought to you by | New York University Bobst Library Technical Services
Authenticated
Download Date | 1/21/16 12:53 PM

TABLE 4. ^{29}Si NMR data for chabazite

Sample	Site	δ (ppm)	/*
CHA001	Si(4Al)	–88.8	0.036
	Si(3Al)	–93.1	0.171
	Si(2Al)	–98.7	0.464
	Si(1Al)	–104.5	0.283
	Si(0Al)	–110.0	0.046
CHA002	Si(4Al)	–88.6	0.093
	Si(3Al)	–93.2	0.249
	Si(2Al)	–98.5	0.425
	Si(1Al)	–104.2	0.209
	Si(0Al)	–109.7	0.023
CHA003	Si(4Al)	–88.3	0.032
	Si(3Al)	–930	0.170
	Si(2Al)	–98.6	0.454
	Si(1Al)	–104.6	0.295
	Si(0Al)	–109.8	0.049
CHA004	Si(4Al)	–88.1	0.012
	Si(3Al)	–92.7	0.124
	Si(2Al)	–98.6	0.467
	Si(1Al)	–104.5	0.336
	Si(0Al)	–109.9	0.061

* Relative intensity (peak area).

range in Si/Al determined by ^{29}Si MAS NMR. The relative direction of the discrepancy is not consistent with an explanation based on the presence of Al-O-Al linkages.

Wairakite

The ^{29}Si MAS NMR spectrum obtained for natural wairakite (ANA004) is shown in Figure 3 along with the provisional fit reported in Table 5. Three prominent signals are present in the spectrum of Figure 3 at –92.9, –95.4, and –97.6 ppm, similar to the spectrum for a synthetic wairakite sample reported by Henderson et al. (1998). All three of these peaks likely represent Si(2Al) sites consistent with the structural model for wairakite presented by Takeuchi et al. (1979). As suggested by Henderson et al. (1998) on the basis of correlations between average T-O-T bond angles and δ for Si(2Al) sites, the –92.9, –95.4, and –97.6 ppm signals probably correspond to ^{29}Si on tetrahedral sites T11B + T12A, T12B, and T11A, respectively (site designations from Takeuchi et al. 1979). The spectrum was fitted assuming pure Gaussian peak shapes and is consistent with the approximate 1:1:1:1 relative intensity of the four Si-dominant sites in wairakite. However, some additional intensity is present that is not associated with the three main signals, particularly on the high frequency (left, as plotted) side of the spectrum. The fit shown in Figure 3 and Table 5 suggests that approximately 15% of the intensity of the spectrum is present at higher frequencies than the T11B + T12A(2Al) peak. The poor resolution of features outside of the three main peaks precluded unique fitting of these portions of the spectrum. The fitting results shown in Table 5 are thus only suggestive of the real distribution of signals and ignores the possible contribution of other signals that are coincident with the region of the three main peaks. Nonetheless, all attempts at fitting the spectrum of Figure 3 indicate that at least 15% of spectrum is due to signals other than Si ordered onto T11A, T11B, T12A, and T12B.

TABLE 5. ^{29}Si NMR data for wairakite (ANA004)

Site*	δ (ppm)	/†
T11B(4Al) + T12A(4Al)	–82.1	0.089
T12B(4Al)	–85.0	0.017
T11B(3Al) + T12A(3Al)	–897.4	0.032
T12B(3Al)	–89.3	0.007
T11B(2Al) + T12A(2Al)	–92.9	0.439
T12B(2Al)	–95.4	0.197
T11A(2Al)	–97.6	0.209
T12B(0Al)	–103.6	0.009

* Site nomenclature after Takeuchi et al. (1979).
† Relative intensity (peak area).

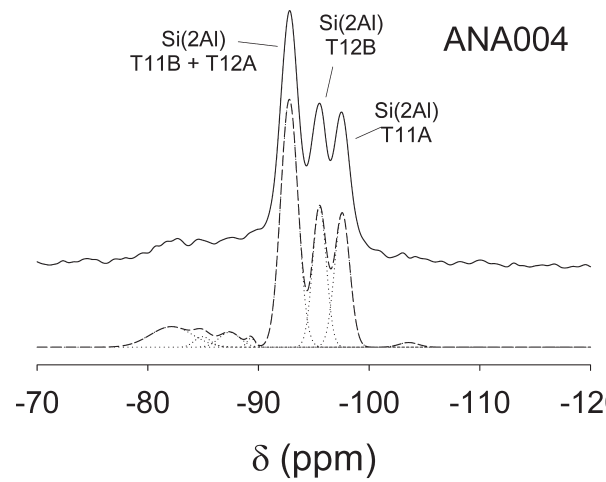

FIGURE 3. ^{29}Si MAS NMR spectra at 9.4 T for wairakite sample ANA004. The upper spectrum is the experimental result and the lower corresponds to the fits listed in Table 5.

DISCUSSION

Disorder and configurational entropies in chabazite and analcime

Based on ^{29}Si MAS NMR studies, chabazite and analcime do not appear to exhibit long range Si-Al order in their tetrahedral frameworks. Structures of both minerals have been refined in space groups that lead to several crystallographically distinct tetrahedral sites (Mazzi and Galli 1978, 1983; Vezzalini et al. 1997; Yokomori and Idaka 1998; Cruciani and Gualtieri 1999); however, the framework topologies of both the CHA and the ANA generic structure types have higher symmetries (rhombohedral and cubic, respectively; Meier et al. 2001) with only one distinct tetrahedral site. However, the ^{29}Si MAS NMR spectra shown above for analcime and chabazite, and those published previously (see below), exhibit signals from only one site. As noted by Murdoch et al. (1988), the lack of resolution of signals from multiple tetrahedral sites in analcime is likely a manifestation of the very similar average T-O-T bond angles for these sites, and the same argument could be made for chabazite. One could argue that the true Si-Al ordering of analcime and chabazite cannot be resolved from ^{29}Si MAS NMR spectra if this is in fact the case. The evidence presented below suggests, however, that the crystallographically distinct tetra-

Brought to you by | New York University Bobst Library Technical Services
Authenticated
Download Date | 1/21/16 12:53 PM

hedral sites in analcime and chabazite may not be energetically distinct, and that consideration of only short range Si-Al disorder is appropriate for assessing the stability of this phase.

In zeolite frameworks with only one tetrahedral site, the problem of characterizing Si-Al configurations in the structure is analogous to that of characterizing magnetic spins. Consequently, numerous attempts have been made to apply the Ising model (originally developed for the problem of describing magnetic spin states) to the description of short-range Si-Al ordering in zeolites (Gordillo and Herrero 1996; Herrero 1990, 1993; Herrero et al. 1991, 1992; Neuhoff and Stebbins 2001; Phillips and Kirkpatrick 1994). The most common method used to characterize local Si-Al configurations described by ^{29}Si MAS NMR spectra is the cluster variation method (CVM; cf. Kikuchi 1951). Phillips and Kirkpatrick (1994) derived a CVM relationship that relates the distribution of Si-Al configurations (Ω) in a tetrahedral framework to the distribution of Si(nAl) and Al(oSi) pentads (where o is the number of Si second nearest neighbors around an Al atom on a tetrahedral site) and the distribution of Si-O-Si, Si-O-Al, and Al-O-Al dyads (all of which can be calculated from ^{29}Si MAS NMR spectra assuming Al avoidance). The resulting relationship is given by

$$\ln\Omega = -\Sigma_i d_{p,i} x_{p,i} \ln x_{p,i} + 2\Sigma_j d_{d,j} x_{d,j} \ln x_{d,j} \quad (2)$$

where i span all possible pentad configurations (p) with degeneracy and probability $d_{p,i}$ and $x_{p,i}$, respectively, and j span all possible dyad configurations (d) with degeneracy and probability $d_{d,j}$ and $x_{d,j}$, respectively. The probabilities of the Si(nAl) pentads ($x_{p,Si(nAl)}$) are given by

$$x_{p,Si(nAl)} = X_{Si} (I_{Si(nAl)}/d_{p,Si(nAl)}) \quad (3)$$

and that of the Al(4Si) pentad ($x_{p,Al(4Si)}$) is equal to X_{Al}. Degeneracy represents the number of different configurations possible for the pentad or dyad; for instance, there are four possible configurations of next nearest neighbor Al and Si around the central Si atom in a Si(3Al) pentad and six around the Si(2Al) pentad. The probabilities of the Si-O-Al and Si-O-Si dyads ($x_{d,Si\text{-}O\text{-}Al}$ and $x_{d,Si\text{-}O\text{-}Si}$, respectively) are equal to X_{Al} and $(1–2X_{Al})$, respectively.

Table 6 summarizes S_{CON} due to short-range disorder for the chabazite samples discussed above calculated using the above method (on the basis of 24 framework O atoms in the CHA unit cell). Also included in Table 6 are the corresponding calculations for all other chabazite samples with reported Si(nAl) distributions from the literature of which we are aware along with data for synthetic zeolite samples with the closely related GME framework. The GME framework, represented in nature by the mineral gmelinite, contains only one tetrahedral site (Vezzalini et al. 1990; Sacerdoti et al. 1995) For comparison, S_{CON} values calculated for these framework compositions that correspond to a purely random Si-Al distribution and that predicted assuming Al avoidance as the only ordering mechanism for these framework compositions (calculated from the equations of Phillips and Kirkpatrick 1994) are also presented in Table 6. It can be seen from the data in Table 6 that all CHA and GME framework materials studied exhibit S_{CON} values significantly less than that predicted for a fully disordered Si-Al distribution. Most of the experimental values in Table 6 approach the theoretical values based on Al avoidance, consistent with this phenomenon being the main source of ordering in these materials.

The experimental S_{CON} data in Table 6 are plotted in Figure 4a (symbols), which illustrates the variation of S_{CON} in chabazite as a function of framework composition (calculated from Eq. 1). Shown for reference in Figure 4a is the S_{CON} predicted assuming Al avoidance is the only ordering mechanism and assuming purely random mixing of Si and Al (curves; cf. Phillips and Kirkpatrick 1994). Taken together, all of the data in Figure 4a define a trend of S_{CON} as a function of X_{Al}. Thus, within the limits of the scatter in the data plotted in Figure 4a (which is in large part due to variations in the quality of spectra and fits obtained in the studies listed in Table 6), it appears that at a given framework composition, the degree of short-range Si-Al ordering is very similar for all of the GME and CHA materials studied, although synthetic chabazite may be more disordered

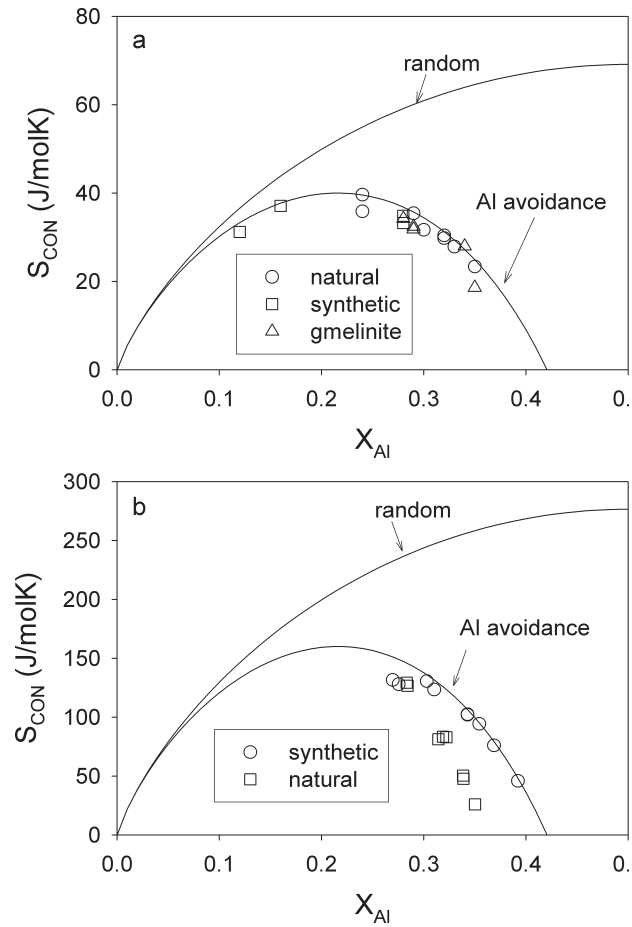

FIGURE 4. Configurational entropies calculated from reported ^{29}Si MAS NMR line intensities (Tables 6 and 7) for CHA and GME structure zeolites on a 24 tetrahedral site basis (**a**) and ANA structure zeolites on a 48 tetrahedral site basis (**b**) as a function of X_{Al}. Shown for comparison are theoretical curves depicting full disorder and pure aluminum avoidance.

Brought to you by | New York University Bobst Library Technical Services
Authenticated
Download Date | 1/21/16 12:53 PM

TABLE 6. Calculated framework compositions and configurational entropies of chabazite and related compounds

Study	Sample	Provenance*	S_{CON}†,‡ (J/mol∞K) Si/Al†	X_{Al}†	Measured	Random	Al avoidance
This study	CHA001	Greenland	2.14	0.32	29.81	62.41	31.58
This study	CHA002	Ireland	1.84	0.35	23.37	64.76	24.24
This study	CHA003	Iceland	2.17	0.32	30.43	62.19	32.08
	CHA004	Iceland	2.37	0.30	31.69	60.68	34.86
B1988§	CHA(Az)	Arizona	3.20	0.24	39.65	54.76	39.66
B1988§	CHA(Ic)	Iceland	1.99	0.33	27.89	63.58	28.47
B1988§	CHA(Cdn)	Nova Scotia	2.48	0.29	35.43	59.80	36.09
B1988§	GME‖	Synthetic	1.98	0.34	28.00	63.66	28.24
A1996§	CHA-1	Synthetic	2.63	0.28	34.84	58.74	37.28
	CHA-2	Arizona	3.09	0.24	35.88	55.48	39.42
	CHA-3	Synthetic	5.12	0.16	37.12	44.44	38.02
	CHA-4	Synthetic	7.65	0.12	31.20	35.73	32.70
N1985§	–	Synthetic	2.63	0.28	33.23	58.70	37.32
TK1995§	–	Japan	2.41	0.29	32.43	60.39	35.29
J1991§	b‖	Synthetic	2.41	0.29	32.43	60.39	35.29
J1991§	c‖	Synthetic	2.52	0.28	34.23	59.51	36.45
J1991§	d‖	Synthetic	2.44	0.29	31.83	60.12	35.67
J1991§	e‖	Synthetic	2.14	0.32	29.81	62.41	31.58
KT2000	–‖	Khazakhstan	1.86	0.35	18.62	64.58	24.97

* Locality names given for natural samples.
† Calculated from ^{29}Si MAS NMR spectrum (see text).
‡ Based on 24 framework O atoms.
§ References: B1988 (Bodart et al. 1988); A1996 (Akporiaye et al. 1996); N1985 (Nagy et al. 1985); TK1995 (Takaishi and Kato 1995); J1991 (Joshi et al. 1991); KT2000 (Kato and Takaishi 2000).
‖ Gmelinite.

than natural chabazite. The variation (and magnitude when normalized to the same number of framework O atoms) in S_{CON} with X_{Al} illustrated in Figure 4a is similar to that observed previously for FAU and LTA structure zeolites (Neuhoff and Stebbins 2001).

Using calculations analogous to those described above, Neuhoff and Stebbins (2001) demonstrated that S_{CON} in FAU and LTA framework zeolites is also a regular function of X_{Al}. Significantly more ^{29}Si MAS NMR data is available for materials with these frameworks over a much wider range of X_{Al} (effectively from 0 to 0.5) which allowed identification of two compositions for which S_{CON} was zero, implying an absence of short-range disorder. The first composition was at $X_{Al} = 0$, for which the framework must be fully ordered as only Si is present at tetrahedral sites. The second composition was at approximately $X_{Al} = 0.417$, corresponding to the point at which five out of every twelve tetrahedral sites was occupied by Al. At this composition, long range ordering develops among the double hexamer rings that make up these frameworks as was suggested previously from Monte Carlo modeling and variations in cell parameters as a function of X_{Al} in these materials (Dempsey et al. 1969; Herrero 1993; Herrero et al. 1991, 1992). This ordering is consistent with the requirement that as the Al content of the framework increases, Al arrangement in meta configurations (with Al and Si atoms alternating in the hexamer rings) is required for Al avoidance (as opposed to the para configuration where Al-bearing tetrahedral can be separated by 2 Si-bearing tetrahedra in a hexamer ring). Values of S_{CON} calculated using the CVM method for FAU and LTA samples with X_{Al} greater than ~0.417 were always negative, illustrating the fact that the assumptions of the Ising model break down when long-range order develops. Samples with X_{Al} greater or less than ~0.417 thus constitute distinct solid solutions for these frameworks. Configurational entropies calculated for compositions where long range ordering did not occur were well represented by the relationship

$$S_{CON} = W(X_{aluminous}\ln X_{aluminous} + X_{siliceous}\ln X_{siliceous}) \quad (4)$$

where W is an empirical fitting parameter and the mol fractions of the aluminous and siliceous end-members are given by

$$X_{aluminous} = 1 - X_{siliceous} = X_{Al}/x^* \quad (5)$$

where x^* is the mol fraction of Al in the aluminous end-member.

Regression of the data for natural chabazite samples in Figure 4a indicate that this framework becomes long-range ordered at the same framework composition as FAU and LTA (i.e., S_{CON} is zero at $X_{Al} = x^* \cong 0.417$), corresponding to a framework composition of $Al_5Si_7O_{24}$. This is consistent with the presence of double hexamer rings in the CHA structure (and that of GME, which appears to follow a similar trend; Fig. 4a). On the basis of Monte Carlo modeling of Si and Al distribution in chabazite, Gordillo and Herrero (1996) concluded that long range ordering of Si and Al develops in chabazite at very similar compositions, being nearly complete at X_{Al} of 0.44 or greater. It is interesting to note that natural chabazite exhibit framework compositions with $0.2 \le X_{Al} \le 0.42$, with the more aluminous boundary corresponding almost exactly to the point at which long range order appears to develop in this framework. Willhendersonite, a natural CHA framework zeolite with $X_{Al} = 0.5$, does occur in nature, but exhibits a triclinic symmetry as opposed to the generally rhombohedral symmetry of chabazite (Peacor et al. 1984) reflecting the long range ordering required by an Si/Al ratio of 1.

Table 7 gives S_{CON} calculations analogous to those described above for the natural analcime samples in this study, as well as

Brought to you by | New York University Bobst Library Technical Services
Authenticated
Download Date | 1/21/16 12:53 PM

TABLE 7. Calculated framework compositions and configurational entropies of analcime

Study	Sample	Provenance*	Si/Al†	X_{Al}†	S_{CON}†,‡ (J/mol·K) Measured	Random	Al avoidance
This study	ANA001	Canada	1.95	0.34	47.70	255.53	110.03
This study	ANA002	Greenland	2.10	0.32	82.91	250.83	123.48
This study	ANA003	California	1.86	0.35	25.90	258.40	99.61
PK1994§	Mt. St. Hilaire	Canada	1.95	0.34	50.46	255.42	110.38
PK1994§	UIUC 1904	? (natural)	2.18	0.31	81.28	248.44	128.99
PK1994§	Barstow	California	2.53	0.28	129.19	237.86	146.01
PK1994§	Mohave	Arizona	2.52	0.28	126.63	238.14	145.67
M1988§	–	Colorado	2.14	0.32	83.34	249.80	125.94
K1995§	–	Synthetic	1.95	0.34	–5.23	255.54	110.00
KH1998§	A	Synthetic	1.55	0.39	45.97	267.25	48.37
KH1998§	B	Synthetic	1.71	0.37	76.08	262.69	79.44
KH1998§	C	Synthetic	1.92	0.34	102.17	256.55	106.54
KH1998§	D	Synthetic	2.22	0.31	123.45	247.12	131.72
KH1998§	E	Synthetic	2.30	0.30	130.63	244.75	136.12
Y1998§	–	Synthetic	1.92	0.34	102.45	256.55	106.57
H1995§	–	Synthetic	1.82	0.35	94.37	259.42	95.35
HK1995§	–	Synthetic	2.63	0.28	128.00	234.87	149.20
J1991§	–	Synthetic	2.71	0.27	131.70	232.62	151.25

* Locality names given for natural samples.
† Calculated from ^{29}Si MAS NMR spectrum (see text).
‡ Based on 96 framework O atoms.
§ References: PK1994 (Phillips and Kirkpatrick 1994); M1988 (Murdoch et al. 1988); K1995 (Kohn et al. 1995); KH1998 (Kato and Hattori 1998); Y1998 (Yamazaki personal communication to Takaishi 1998); H1998 (He et al. 1995); HK1995 (Herreros and Klinowski 1995); J1991 (Joshi et al. 1991).

those of natural and synthetic analcime samples reported in the literature (calculated on the basis of 48 tetrahedral sites). Note that the calculations for the samples of Murdoch et al. (1988) and Phillips and Kirkpatrick (1994) were previously reported by the latter authors. The data of Table 7 are plotted in Figure 4b, again with theoretical lines for S_{CON} assuming random Si-Al distributions and Al avoidance. As seen in Figure 4b, the data for analcime appear to define two trends, one composed entirely of synthetic samples that closely follows the Al avoidance curve and another, composed largely of natural samples, that exhibits significantly lower degrees of Si-Al disorder (i.e., lower values of S_{CON} for a given composition). These trends are subsequently referred to as the synthetic and natural trends, respectively. The synthetic samples listed in Table 5 were synthesized by a wide variety of methods under different conditions. This may account for the fact that the samples prepared by Herreros and Klinowski (1995) and Joshi et al. (1991) follow a different trend (that of the natural samples) than the other synthetic samples. This is the first example we are aware of in which a single material exhibits two distinct states of *short-range* Si-Al ordering. Of special note is the sample reported by Kohn et al. (1995) for which the calculated S_{CON} is negative, implying that this sample is long-range ordered (see discussion in Neuhoff and Stebbins 2001). This result may in part reflect the fact that the data used in the calculation were from a cross polarization experiment (and thus not truly quantitative); however, visual inspection of their single pulse ^{29}Si MAS NMR spectrum supports the conclusion that this sample is anomalously ordered and may represent yet a third state of ordering in analcime beyond those of the two trends in Figure 4b.

Fitting of the analcime data in Figure 4b to Equation 4 indicates that x^* for the synthetic and natural zeolite trends corresponds to X_{Al} values of ~0.417 and 0.357, respectively. The former value is essentially identical to that found for CHA, FAU, and LTA zeolites, and suggests that this set of samples develops long-range ordering when linked pairs of hexamer rings making up the ANA framework reach a collective Al content of 5 out of 12 tetrahedral sites (and thus Si and Al must alternate between sites in the two rings in a meta configuration). This behavior is analogous to that of the double six rings in CHA, FAU, and LTA. The composition at which the natural sample array develops long range ordering is very similar to a composition with 17 Al atoms for every 48 tetrahedral sites (X_{Al} = 0.354). At this degree of Al loading, development of meta configurations in hexamer rings is required in the unit cell for analcime (which contains 48 tetrahedral sites).

The presence of two (and perhaps three) trends in Figure 4b suggests that different short range ordering mechanisms are possible in this structure. The similarity between the Al avoidance curve and the synthetic trend suggests that this is the main short range ordering mechanism in this array. The samples in the natural trend are significantly more ordered than required by Al avoidance alone, as noted by Phillips and Kirkpatrick (1994). Although Takaishi (1998) rejected minimization of Al-O-Si-O-Al linkages as a short-range ordering mechanism in analcime (i.e., Dempsey's rule; Dempsey et al. 1969), it appears, as Phillips and Kirkpatrick (1994) concluded, that natural analcime samples are ordered in such a way as to minimize these linkages. This can be demonstrated from a moment analysis (cf. Vega 1983) of the data for the samples in Table 7 which indicates that the density of Al-O-Si-O-Al linkages is lower for the natural array than for the synthetic array. The sample studied by Kohn et al. (1995) has an even lower Al-O-Si-O-Al density than the natural array.

Natural analcime samples (mostly from low-grade metamorphic and diagenetic environments) typically have X_{Al} between 0.26 and 0.34. The only exceptions to this are samples of potentially primary igneous analcime from theralites, which exhibit an X_{Al} of 0.4 (Wilkinson and Hansel 1994). This X_{Al} is larger than x^* for the natural array, which suggests that these samples are either long range ordered, or exhibit a greater degree of short range disorder than metamorphic and diagenetic

Brought to you by | New York University Bobst Library Technical Services
Authenticated
Download Date | 1/21/16 12:53 PM

analcime samples and potentially fall along the synthetic curve in Figure 4b. The latter conclusion would be consistent with a higher temperature of formation for primary igneous analcime. Characterization of such samples by ^{29}Si MAS NMR would prove very interesting. If the latter case were true, it would support the conclusion of Kim and Burley (1980) that analcime undergoes a phase transition to a more disordered phase at high temperatures.

A series of papers have demonstrated distributions of Si and Al in the unit cells of the GME, CHA, and ANA framework that lead to Si(nAl) pentad distributions consistent with those of the chabazite and synthetic analcime trends of Figure 4 (Kato and Hattori 1998; Kato and Takaishi 2000; Takaishi and Kato 1995). Although both the present and earlier works primarily use Al avoidance as a constraint on the distribution of Si and Al in the lattices, this study only considers connectivity at the level of a pentad in constraining tetrahedral cation configurations whereas unit-cell-scale connectivity relations were taken into account by the previous authors. Facially, the conclusions of the present study appear at odds with the contentions of Kato and Hattori (1998), Kato and Takaishi (2000), and Takaishi and Kato (1995) that Si and Al are long-range "ordered" over the unit cells of these materials: the positive values of S_{CON} calculated above inherently imply long-range and short-range disorder. However, as noted by these authors, the "ordered" configurations determined in their work are not unique; in fact, numerous equivalent configurations are possible because of the high symmetries of the GME, ANA, and CHA structure types. Distribution of these equivalent configurations among unit cells in a sample would actually represent long-range disorder, which, as Kato and Takaishi (2000) noted, is a probable explanation for the fact that space groups implied by structural refinements for these materials tend to have higher degrees of symmetry than those determined for individual "ordered" unit cells.

Energetics of framework solid solutions in chabazite and analcime

The S_{CON} data presented in Figures 4a and 4b and Tables 6 and 7 are recast in Figure 5 as a function of the mol fractions of the aluminous end-members (calculated assuming x^* corresponds to 5 Al atoms out of every 12 tetrahedral sites for natural chabazite and synthetic analcime solid solutions and 17 Al atoms in every 48 tetrahedral sites for natural analcime) for the three solid solutions discussed above. Note that a mol fraction of 0 for each of these solid solutions corresponds to a pure silica framework, following the treatment of Neuhoff and Stebbins (2001) for FAU and LTA zeolite samples. Purely siliceous framework compositions are unknown in the ANA framework, and are thus hypothetical. Purely siliceous chabazite has been synthesized (Woodcock et al. 1999) but is not known in natural parageneses and is thus also hypothetical. The data in Figure 5 were regressed to Equation 4. The corresponding values of W are –56.0 J/(mol·K) for natural chabazite ($R^2 = 0.940$), –256.6 J/(mol·K) for natural analcime ($R^2 = 0.975$), and –219.0 for synthetic analcime ($R^2 = 0.995$).

Shown for comparison in Figure 5 are the corresponding curves for the ideal configurational entropy of mixing for these solid solutions, $S_{CON,ideal}$, as a function of $X_{aluminous}$ which was

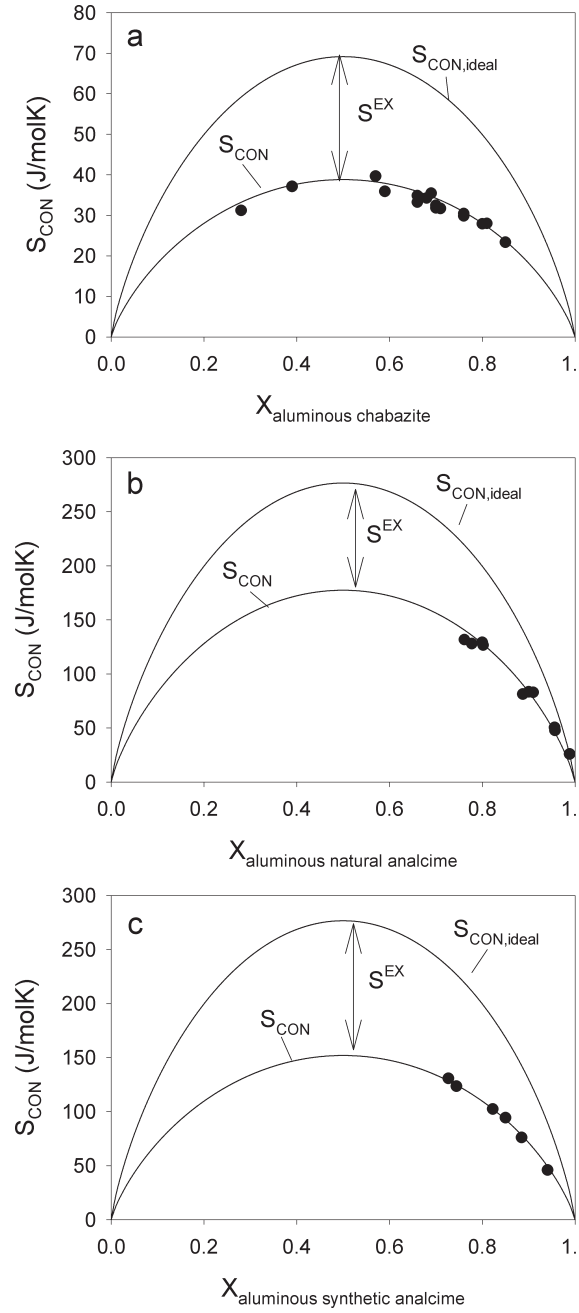

FIGURE 5. Configurational entropies for chabazite (**a**), natural analcime (**b**) and synthetic analcime (**c**) solid solutions as a function of the mol fraction of the aluminous end-member (see text for details). Curve labeled "S_{CON}" is a regression of the experimental data to Equation 2. Curve labeled "$S_{CON,ideal}$" represents the ideal configurational entropy arising from mixing between the aluminous siliceous end-members for each solid solution.

calculated from the expression

$$S_{CON,ideal} = -mR\Sigma_k X_k \ln X_k \quad (6)$$

where subscripts k denote the compositional end-members in

Brought to you by | New York University Bobst Library Technical Services
Authenticated
Download Date | 1/21/16 12:53 PM

the solid solution and m is the number of tetrahedral sites in the molar formula used for the calculations (m = 48 for analcime and m = 12 for chabazite). Assuming the absence of an excess calorimetric contribution to the entropy (S) of these zeolites (which seems reasonable given the general success of oxide summation algorithms for predicting S in zeolite samples of variable composition; Neuhoff 2000), the difference between the regressed (S_{CON}) and $S_{CON,ideal}$ curves in Figures 5a–c represents the excess entropy of mixing (S^{EX}) in these solid solutions (cf. Neuhoff and Stebbins 2001):

$$S^{EX} = S_{CON} - S_{CON,ideal} \quad (7)$$

Note that the excess entropy is negative. Combining Equations 4, 6, and 7 leads to:

$$S^{EX} = W(\Sigma_k X_k \ln X_k) + nR(\Sigma_k X_k \ln X_k) \quad (8)$$

The excess Gibbs energy of mixing (G^{EX}) for a composition within a solid solution is given by:

$$G^{EX} = H^{EX} - TS^{EX} \quad (9)$$

where H^{EX} is the excess enthalpy of mixing. Enthalpies of formation (ΔH_f) determined for hydrated and dehydrated chabazites (X_{Al} between 0.27 and 0.49) by lead borate drop solution calorimetry are nearly linear functions of X_{Al} (Shim et al. 1999). This suggests that H^{EX} for Si-Al substitution in chabazite is negligible. The ΔH_f data currently available for analcime cover too small a range in composition to make a similar analysis. However, negligible H^{EX} for Si-Al substitution in zeolites appears to be quite common, being observed not only in chabazite, but also faujasite (Neuhoff and Stebbins 2001; Petrovic and Navrotsky 1997) and is consistent with the behavior of stilbite-stellerite solid solutions (Fridriksson et al. 2001). It is thus assumed that $H^{EX} = 0$ for all of the solid solutions considered here. As a consequence of this assumption, Equation 9 reduces to:

$$G^{EX} = -T^* S^{EX} \quad (10)$$

The activities of the end-members in these solid solutions are given by

$$a_k = (X_k \gamma_k)^n \quad (11)$$

where γ_k is the activity coefficient and the exponent accounts for the stoichiometry of tetrahedral sites. The activity coefficients can be assessed through the equations above by noting that

$$RT\ln\gamma_k = G^{EX} - (1 - X_k)[\delta G^{EX}/\delta(1 - X_k)]_{T,P,X_k} \quad (12)$$

where the right hand side is an expression of the partial molar Gibbs energy of mixing of end-member k. Combination and rearrangement of Equations 8, 10, and 12 leads to an explicit expression for γ_k:

$$\ln\gamma_k = -(W/R + m)\ln(X_k) \quad (13)$$

Note that γ_k is not a function of temperature as a consequence of the assumption $H^{EX} = 0$ (i.e., an athermal solution). The consequences of this type of solid solution are discussed by Neuhoff and Stebbins (2001).

Validity of S_{CON} calculations

The magnitudes of the S_{CON} values calculated above suggest that short-range disorder can have a significant effect on the energetics of analcime and chabazite. For instance, calorimetrically determined ("Third Law") entropies for analcime and chabazite at 298.15 K ($S_{298.15}$) are approximately 3600 J/(mol·K) (on a 96 framework O atom basis; Johnson et al. (1982) and 1200 J/(mol·K) (on a 24 framework O atom basis; Belitsky et al. 1982), respectively. The actual entropies of these materials at 298.15 K (S), are given by the relationship

$$S = S_{298.15} + S_{CON} \quad (14)$$

assuming no entropic contribution from phase transitions below 298.15 K. Thus, the configurational entropies of chabazite and analcime (cf. Tables 6 and 7) add an additional 1 to 4% to their entropies at 298.15 K. Given the relatively small entropies of reactions governing many zeolite phase relations, this increase in $S_{298.15}$ can have a disproportionately large effect on calculated equilibria. However, to our knowledge, the validity of the quantitative results of CVM calculations for framework silicates have not been rigorously tested, which requires an independent observation of the configurational entropy of these materials. Analcime presents an opportunity to test the validity of the S_{CON} calculations described above. Figure 6 shows experimental observations by J.J. Hemley (cited as a personal communication to Helgeson et al. 1978 and tabulated in Johnson et al. 1982) of the activity of aqueous silica ($a_{SiO2,aq}$) in equilibrium with ordered albite and analcime (latter from lava flows on Table Mountain, Colorado, the same locality and sample composition as the sample of Murdoch et al. 1988 listed in Table 7). Based on the composition of the analcime in these experiments, these observations pertain to the reaction

$$\underset{\text{analcime}}{Na_{15.36}Al_{15.36}Si_{32.64}O_{96}\cdot 16H_2O} + 13.44\ SiO_{2,aq} = 15.36\ \underset{\text{low albite}}{NaAlSi_3O_8} + 16\ H_2O \quad (15)$$

These observations present a unique opportunity for assessing the magnitude of S_{CON} in analcime, as the heat capacity and calorimetrically determined entropy of analcime of this composition were measured by Johnson et al. (1982), which as shown below permits direct determination of S_{CON} for analcime from the temperature dependence of the data in Figure 6.

The curves in Figure 6 were calculated with the aid of the SUPCRT92 software package (Johnson et al. 1992; see also Helgeson et al. 1978). Thermodynamic data for low albite, water, and aqueous silica were taken from the SUPCRT92 database. The temperature dependence of the heat capacity [C_p(J/mol·K) = 2111.5 + 4.098 T + 3949000 T^{-2}] and $S_{298.15}$ [3628 J/(mol·K)] were calculated from the calorimetric data of

Brought to you by | New York University Bobst Library Technical Services
Authenticated
Download Date | 1/21/16 12:53 PM

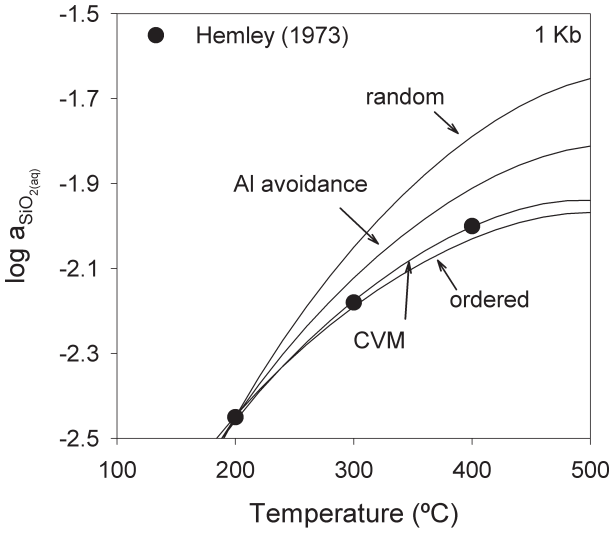

FIGURE 6. Calculated effects of various disorder models on the stability of analcime. The experimental data from Hemley (1973; personal communication to Helgeson et al. 1978) pertain to the activity of aqueous silica ($SiO_{2,aq}$) in equilibrium with albite and analcime as a function of temperature at 1 kb. The curves correspond to calculated equilibrium compositions of $SiO_{2,aq}$ in equilibrium with these minerals assuming different values of S_{CON}. See text for details of the calculations.

Johnson et al. (1982). The molar volume (1548 cm^3/mol) was assumed independent of temperature and pressure and was calculated from the determinative curves of Coombs and Whetten (1967). The curves in Figure 6 differ in the magnitude of S_{CON} assumed in the calculations and correspond to values of 0 J/(mol·K) (i.e., assuming that Si and Al are fully ordered; curve labeled "ordered"), 81.92 J/(mol·K) (calculated from the experimental data of Murdoch et al. 1988; curve labeled "CVM"), 125.92 J/(mol·K) (assuming maximum disorder complying with Al avoidance; curve labeled "Al avoidance") and 249.76 J/(mol·K) (assuming random Si-Al distribution; curve labeled "random"). The Gibbs energy of formation (ΔG_f) from the elements and ΔH_f were arbitrarily adjusted so that each curve passed through the data point at 200 °C, 1 kb.

Figure 6 shows that the magnitude of S_{CON} chosen for analcime has a dramatic effect on the calculated temperature dependence of $a_{SiO2,aq}$ in equilibrium with Table Mountain analcime and low albite. Assuming that analcime is fully ordered leads to an underestimation of the temperature dependence of $a_{SiO2,aq}$, whereas assuming Al avoidance alone or a completely random Si-Al distribution leads to a significantly greater temperature dependence than indicated by Hemley's data. In contrast, S_{CON} calculated using Equation 2 leads to a calculated curve that is in excellent agreement with the experimental results. This suggests that the methodology of Equation 2 leads to values of S_{CON} that are consistent with the thermodynamic behavior of this phase and in part validates this method. The apparent validity of the S_{CON} calculations for the Table Mountain analcime sample is further supported by the fact that ΔH_f consistent with the curve labeled "CVM" in Figure 6 (–52738 kJ/mol) is within error of the calorimetric determinations by Barany (1962; recalculated by Johnson et al. 1982 to be –52774 ± 42 kJ/mol) and Johnson et al. (1982; –52750 ± 53 kJ/mol) on samples of the same composition (the sample used by Barany 1962 was from Table Mountain). The fact that it appears that only Si-Al distribution need be considered in assessing S_{CON}, as opposed to consideration of the occupancy of Na sites, may reflect the fact that Na and water site occupancy is inherently linked through charge balance constraints to the presence of Al.

Alberti (1991), using the method of Alberti and Gottardi (1988), calculated the distribution of Si and Al across two tetrahedral sites in analcime from structural refinements of seven analcime samples reported by Mazzi and Galli (1978). His results suggest that different analcime samples vary widely in the degree of long-range Si-Al ordering across sites. Configurational entropies arising from the distribution of Si and Al across the T1 and T2 sites in analcime were calculated from Alberti's (1991) results via the standard expression for S_{CON} arising from long range disorder:

$$S_{con} = -R\sum_i n\sum_j X_{i,j} \ln X_{i,j} \quad (16)$$

where the summation is over all sites i having a multiplicity of n in the structure and all species j (i.e., Si and Al) at the site. The values of S_{CON} calculated in this manner ranged from 12.9 to 15.4 J/(mol·K), nearly as large as that calculated assuming random mixing of Si and Al. This would lead to a curve similar to the one labeled "random" in Figure 6. It thus appears that S_{CON} derived from estimates of long range order in analcime do not accurately reflect the energetics of disordering.

Recently, Cheng et al. (2000) presented ^{17}O MAS NMR and triple quantum (3Q) MAS NMR data that demonstrated the presence of ca. 4% Al-O-Al dyads in a sample of analcime from Table Mountain. This clearly in conflict with the assumption of perfect Al avoidance used in the above calculations. The energetic consequences of Cheng et al.'s (2000) observations are difficult to quantify using Equation 2, as no information is available to assess the relative abundances of Al-centered pentads in the absence of Al avoidance. Nonetheless, it seems likely that the presence of additional Al(nSi) pentads will increase the entropy of analcime above that calculated by applying Equation 2 with the assumption of Al avoidance. It is possible to calculate an S_{CON} value arising from the distribution of dyads in the structure by using the equations of Phillips and Kirkpatrick (1994). The result is ~11.1 J/(mol·K), which would lead to a curve plotting between the "Al avoidance" and "random" curves in Figure 6 that thus overestimates the temperature dependence of $a_{SiO2,aq}$ in equilibrium with analcime and albite. These dyads are not present in ANA001 (Zhao et al. 2001) and the essentially exact correspondence between the Si/Al ratio determined from the original ^{29}Si MAS NMR data and chemical analyses of Murdoch et al. (1988) for analcime from the same location as the sample of Cheng et al. (2000) both strongly support Al avoidance. It is possible that the presence of Al-O-Al dyads was induced during initial high-temperature dehydration (prior to ^{17}O-enrichment) of Cheng et al.'s sample. This change may have gone undetected in their study

Brought to you by | New York University Bobst Library Technical Services
Authenticated
Download Date | 1/21/16 12:53 PM

as all ^{29}Si MAS NMR peaks were broadened by the heating process. In addition, the anomalously small quadrupolar coupling constant for the observed Al-O-Al peak in the ^{17}O-exchanged analcime may have exaggerated its intensity to an extent greater than that originally estimated. Nevertheless, more work is clearly needed to address the degree to which Al avoidance is present in analcime.

Disorder in wairakite

The ^{29}Si MAS NMR spectrum obtained for wairakite clearly illustrates long-range Si-Al ordering in this material, as suggested previously (Henderson et al. 1998; Takeuchi et al. 1979). The specimen investigated in the present study, as well as those studied by Takeuchi et al. (1979) and Henderson et al. (1998) are all monoclinic, with the low symmetry being a consequence of the large degree of Si-Al ordering. Numerous studies have synthesized tetragonal wairakites (Liou 1970), often referred to as Ca-analcimes. Although to our knowledge no spectroscopic or diffraction studies have been performed on such material, it would appear likely that Liou's (1970) conclusion that tetragonal wairakite (Ca-bearing analcime) is Si-Al disordered, leading to the higher symmetry, is correct. Liou (1970) synthesized tetragonal wairakite and then transformed it to monoclinic wairakite by isothermal-isobaric treatment at temperatures of 300 to 400 °C indicating that the disordered form is metastable in this temperature range. This is noteworthy because this temperature range includes the probable maximum thermodynamic stability limit for wairakite. Coombs (1955) suggested that the lamellar twinning often observed in wairakite is a consequence of a transition from a nominally cubic, high temperature phase to the monoclinic phase observed at room temperature. If this is true, the transition probably did not arise from ordering of Si and Al upon cooling, but rather, as Coombs (1955) suggested, was due to the non-quenchable and rapid transition similar to that in leucite and other materials that share the ANA framework (Hovis et al. 2002; Kohn et al. 1997; Xu et al. 2001).

Liou (1970) suggested that the spacing between the 004 and 400 reflections in wairakite (effectively the difference in the *a* and *c* unit-cell dimensions) increases with increasing order. This appears to be qualitatively consistent with the ^{29}Si MAS NMR data gathered to date for wairakite. The *a*-*c* difference in sample ANA004 from the original batch of starting materials was reported to be 0.09 (Liou 1970). The equivalent value for the synthetic sample studied by Henderson et al. (1998) is 0.118 (T. Bell, personal communication, 2000), making their sample considerably more ordered than ANA004 or any produced by Liou (1970) even during much longer experimental runs. The ^{29}Si MAS NMR spectrum for Henderson et al.'s (1998) sample revealed somewhat less disorder than the natural sample in this study, with only ~10% of the signal lying on the high frequency side of the main peaks whereas in our sample ~15% of the total signal was in this region. Assuming that *a*-*c* does reflect the degree of disorder, comparison of the results summarized above and other *d*-spacings reported in the literature (Aoki and Minato 1980; Takeuchi et al. 1979) suggest that a range of ordering states are present in natural and synthetic wairakite. Indeed, most of the samples studied by Aoki and Minato (1980) have *a*-*c* values that are greater than those of Henderson et al.'s (1998) sample and thus likely exhibit greater degrees of Si-Al order.

As Liou (1970) demonstrated, disordered wairakite samples can represent metastable states. However, the possibility remains open that some of the variation in Si-Al ordering in wairakite suggested by reported unit-cell parameters may reflect significant temperature-dependent equilibrium disordering in the range of temperature and pressure over which this phase forms in natural and laboratory systems. The significantly lower ordering state for Liou's (1970) starting material (and apparently his run products, which never exceeded this ordering state) than most of the natural samples studied by Aoki and Minato (1980) suggests that the equilibria determined in his study may be metastable, or at least not directly comparable to equilibria involving most natural wairakite samples.

Acknowledgments

This work was supported by the U.S. National Science Foundation (grant EAR-0104926 to J.F.S. and EAR-0001113 to D.K.B.) and the Petroleum Research Fund (grant ACS-PRF 31742-AC2 to D.K.B.). Th. Fridriksson, A. Spieler, and R. Jones are thanked for assistance with the electron microprobe analyses, along with T. Kiczenski for assistance with collection of XRPD data. T. Bell is thanked for provided unpublished XRD data on wairakite. J.-G. Liou and S. Kleine generously donated samples for this study. Additional samples used in this study were collected on expeditions funded by the Stanford McGee Fund, the Danish Lithosphere Centre, and the Geological Survey of Denmark and Greenland.

References cited

Akporiaye, D.E., Dahl, I.M., Mostad, H.B., and Wendelbo, R. (1996) Aluminum distribution in chabazite: An experimental and computational study. Journal of Physical Chemistry, 100, 4148–4153.

Alberti, A. (1991) Crystal Chemistry of silicon-aluminum distribution in natural zeolites. In T. Inui, S. Namba, and T. Tatsumi, Eds., Chemistry of microporous crystals: proceedings of the International Symposium on Chemistry of Microporous Crystals. Studies in Surface Science and Catalysis, 60, p. 107–122. Elsevier, Amsterdam.

Alberti, A. and Gottardi, G. (1988) The determination of the Al-content in the tetrahedra of framework silicates. Zeitschrift Fur Kristallographie, 184, 49–61.

Aoki, M. and Minato, H. (1980) Lattice constants of wairakite as a function of chemical composition. American Mineralogist, 65, 1212–1216.

Barany, R. (1962) Heats and free energies of formation of some hydrated and anhydrous sodium- and calcium-aluminum silicates. Bureau of Mines Report of Investigations 5900, 17 p.

Belitsky, I.A., Gabuda, S.P., Drebushchak, V.A., Naumov, V.N., Nogteva, V.V., and Paukov, I.E. (1982) Heat capacity of chabazite in the temperature range of 5 to 316K, entropy and enthalpy at standard conditions. Geokhimiya, 1982, 444–446.

Bodart, P., Nagy, J.B., Gabelica, Z., and Derouane, E.G. (1988) High resolution magic-angle-spinning solid state ^{29}Si-NMR characterization of the structure and aluminum orderings in natural and synthetic zeolites of the chabazite group. In D. Kallo and H.S. Sherry, Eds. Occurrence, properties and utilization of natural zeolites, p. 245–255. Akad. Kiado, Budapest.

Cheng, X., Zhao, P.D., and Stebbins, J.F. (2000) Solid state NMR study of oxygen site exchange and Al-O-Al site concentration in analcime. American Mineralogist, 85, 1030–1037.

Chipera, S.J. and Apps, J.A. (2001) Geochemical stability of natural zeolites. In D.L. Bish and M. D.W., Eds. Natural Zeolites: Occurence, Properties, Applications, p. 117–161. Reviews in Mineralogy and Geochemistry, Mineralogical Society of America and the Geochemical Society, Washington, D.C.

Colella, C., de' Gennaro, M., and Aiello, R. (2001) Use of zeolitic tuff in the building industry. In D.L. Bish and D.W. Ming, Eds., Natural Zeolites: Occurence, Properties, Applications, p. 551–587. Reviews in Mineralogy and Geochemistry, Mineralogical Society of America and the Geochemical Society, Washington, D.C.

Coombs, D.S. (1955) X-ray observations on wairakite and non-cubic analcime. Mineralogical Magazine, 30, 699–708.

Coombs, D.S. and Whetten, J.T. (1967) Composition of analcime from sedimentary and burial metamorphic rocks. Geological Society of America Bulletin, 78, 269–282.

Cruciani, G. and Gualtieri A. (1999) Dehydration dynamics of analcime by *in situ* synchrotron powder diffraction. American Mineralogist, 84, 112–119.

Dempsey, E., Kühl, G.H., and Olson, D.H. (1969) Variation of the lattice parameter

Brought to you by | New York University Bobst Library Technical Services
Authenticated
Download Date | 1/21/16 12:53 PM

with aluminum content in synthetic sodium faujasites. Evidence for ordering of the framework ions. Journal of Physical Chemistry, 73, 387–390.
Engelhardt, G. and Michel, D. (1987) High-resolution solid-state NMR of silicates and zeolites. 485 p. Wiley, New York.
Fridriksson, T., Neuhoff, P.S., Arnorsson, S., and Bird, D.K. (2001) Geological constraints on the thermodynamic properties of the stilbite-stellerite solid solution in low-grade metabasalts. Geochimica Et Cosmochimica Acta, 65, 3993–4008.
Gordillo, M.C. and Herrero, C.P. (1996) Al,Si ordering in chabazites: A Monte Carlo study. Chemical Physics, 211, 81–90.
He, H.Y., Cheng, C.F., Seal, S., Barr, T.L., and Klinowski, J. (1995) Solid-state NMR and ESCA studies of the framework aluminosilicate analcime and its gallosilicate analog. Journal of Physical Chemistry, 99, 3235–3239.
Helgeson, H.C., Delany, J.M., Nesbitt, H.W., and Bird, D.K. (1978) Summary and critique of the thermodynamic properties of rock-forming minerals. American Journal of Science, 278A, 1–229.
Henderson, C.M.B., Bell, A.M.T., Kohn, S.C., and Page, C.S. (1998) Leucite-pollucite structure-type variability and the structure of a synthetic end-member calcium wairakite ($CaAl_2Si_4O_{12}\cdot 2H_2O$). Mineralogical Magazine, 62, 165–178.
Herrero, C.P. (1990) Configurational entropy of the Si, Al distribution in zeolites. Chemical Physics Letters, 171, 369–372.
———(1993) Atom ordering in the tetrahedral framework of zeolite A. Journal of Physics, Condensed Matter, 5, 4125–4136.
Herrero, C.P., Utrera, L., and Ramirez, R. (1991) Long-range versus short-range Si, Al ordering in zeolite X and zeolite Y. Chemical Physics Letters, 183, 199–203.
———(1992) Statistical thermodynamics of Si,Al ordering in aluminosilicate faujasites. Physical Review B, 46, 787–794.
Herreros, B. and Klinowski, J. (1995) Hydrothermal synthesis of zeolites from 5-coordinate silicon compounds. Journal of Physical Chemistry, 99, 1025–1029.
Hovis, G.L., Roux, J., and Rodrigues, E. (2002) Thermodynamic and structural behavior of analcime-leucite analogue systems. American Mineralogist, 87, 523–532.
Johnson, G.K., Flotow, H.E., Ohare, P.A.G., and Wise, W.S. (1982) Thermodynamic studies of zeolites—Analcime and dehydrated analcime. American Mineralogist, 67, 736–748.
——— (1983) Thermodynamic studies of zeolites—Natrolite, mesolite and scolecite. American Mineralogist, 68, 1134–1145.
Johnson, J.W., Oelkers, E.H., and Helgeson, H.C. (1992) SUPCRT92—A software package for calculating the standard molal thermodynamic properties of minerals, gases, aqueous species, and reactions from 1 bar to 5000 bar and 0 °C to 1000 °C. Computers and Geosciences, 18, 899–947.
Joshi, P.N., Thangaraj, A., and Shiralkar, V.P. (1991) Studies on zeolite transformation of high-silica gmelinite into analcime. Zeolites, 11, 164–168.
Kallo, D. (2001) Applications of natural zeolites in water and wastewater treatment. In D.L. Bish and D.W. Ming, Eds. Natural Zeolites: Occurence, Properties, Applications, p. 519–550. Reviews in Mineralogy and Geochemistry, Mineralogical Society of America and the Geochemical Society, Washington, D.C.
Kato, M. and Hattori, T. (1998) Ordered distribution of aluminum atoms in analcime. Physics and Chemistry of Minerals, 25, 556–565.
Kato, M. and Takaishi, K. (2000) Ordered distribution of aluminum atoms in a gmelinite framework. Journal of Physical Chemistry B, 104, 4074–4079.
Kikuchi, R. (1951) A theory of cooperative phenomena. Physical Review, 81, 988–1003.
Kim, K.T. and Burley, B.J. (1980) A further study of analcime solid solutions in the system $NaAlSi_3O_8$-$NaAlSiO_4$-H_2O, with particular note of an analcime phase transformation. Mineralogical Magazine, 43, 1035–1045.
Kiseleva, I., Navrotsky, A., Belitsky, I.A., and Fursenko, B.A. (1996) Thermochemistry and phase equilibria in calcium zeolites. American Mineralogist, 81, 658–667.
Klinowski, J., Ramdas, S., Thomas, J.M., Fyfe, C.A., and Hartman, J.S. (1982) A re-examination of Si, Al ordering in zeolites NaX and NaY. Journal of the Chemical Society-Faraday Transactions Ii, 78, 1025–1050.
Kohn, S.C., Henderson, C.M.B., and Dupree, R. (1995) Si-Al order in leucite revisited—New information from an analcite-derived analog. American Mineralogist, 80, 705–714.
———(1997) Si-Al ordering in leucite group minerals and ion-exchanged analogues: An MAS NMR study. American Mineralogist, 82, 1133–1140.
Liou, J.G. (1970) Synthesis and stability relation of wairakite $CaAl_2Si_4O_{12}\cdot 2H_2O$. Contributions to Mineralogy and Petrology, 27, 259–282.
———(1971a) Analcime equilibria. Lithos, 4, 389–402.
———(1971b) P-T stabilities of laumontite, wairakite, lawsonite, and related minerals in the system $CaAl_2Si_2O_8$-SiO_2-H_2O. Journal of Petrology, 12, 379–411.
———(1971c) Stilbite-laumontite equilibrium. Contributions to Mineralogy and Petrology, 31, 171–177.
Lippmaa, E., Magi, M., Samoson, A., Tarmak, M., and Engelhardt, G. (1981) Investigation of the structure of zeolites by solid-state high-resolution ^{29}Si NMR Spectroscopy. Journal of the American Chemical Society, 103, 4992–4996.
Mazzi, F. and Galli, E. (1978) Is each analcime different? American Mineralogist, 63, 448–460.
———(1983) The tetrahedral framework of chabazite. Neues Jahrbuch fuer Mineralogie. Monatshefte, 1983, 461–480.
Meier, W., Olson, D., and Baerlocher, C. (2001) Atlas of zeolite structure types, Fifth Revised Edition. 302 p. Elsevier, Amsterdam.
Ming, D.W. and Allen, E.R. (2001) Use of natural zeolites in agronomy, horticulture, and environmental soil remediation. In D.L. Bish and D.W. Ming, Eds., Natural Zeolites: Occurence, Properties, Applications, p. 619–654. Reviews in Mineralogy and Geochemistry, Mineralogical Society of America and the Geochemical Society, Washington, D.C.
Murdoch, J.B., Stebbins, J.F., Carmichael, I.S.E., and Pines, A. (1988) A ^{29}Si nuclear magnetic resonance study of silicon-aluminum ordering in leucite and analcite. Physics and Chemistry of Minerals, 15, 370–382.
Murphy, W.M., Pabalan, R.T., Prikryl, J.D., and Goulet, C.J. (1996) Reaction kinetics and thermodynamics of aqueous dissolution and growth of analcime and Na-clinoptilolite at 25 °C. American Journal of Science, 296, 128–186.
Nagy, J.B., Engelhardt, G., and Michel, D. (1985) High-resolution NMR on adsorbate-adsorbent systems. Advances in Colloid and Interface Science, 23, 67–128.
Neuhoff, P.S. (2000) Thermodynamic Properties and Parageneses of Rock-Forming Zeolites, 240 p. Ph.D. thesis, Stanford University, Stanford, California.
Neuhoff, P.S., Fridriksson, T., and Bird, D.K. (2000) Zeolite parageneses in the north Atlantic igneous province: Implications for geotectonics and groundwater quality of basaltic crust. International Geology Review, 42, 15–44.
Neuhoff, P.S., Kroeker, S., Du, L.-S., Fridriksson, T., and Stebbins, J.F. (2002) Order/disorder in natrolite group zeolites: A ^{29}Si and ^{27}Al MAS NMR study. American Mineralogist, 87, 1307–1320.
Neuhoff, P.S. and Stebbins, J.F. (2001) A solid solution model for Si-Al substitution in disordered FAU and LTA zeolites. Microporous and Mesoporous Materials, 49, 139–148.
Peacor, D.R., Dunn, P.J., Simmons, W.B., Tillmanns, E., and Fischer, R.X. (1984) Willhendersonite, a new zeolite isostructural with chabazite. American Mineralogist, 69, 186–189.
Petrovic, I. and Navrotsky, A. (1997) Thermochemistry of Na-faujasites with varying Si/Al ratios. Microporous Materials, 9, 1–12.
Phillips, B.L. and Kirkpatrick, R.J. (1994) Short-range Si-Al order in leucite and analcime—Determination of the configurational entropy from ^{27}Al and variable temperature ^{29}Si NMR spectroscopy of leucite, its Cs-exchanged and Rb-exchanged derivatives, and analcime. American Mineralogist, 79, 1025–1031.
Redkin, A.F. and Hemley, J.J. (2000) Experimental Cs and Sr sorption on analcime in rock-buffered systems at 250–300 °C and P_{sat} and the thermodynamic evaluation of mineral solubilities and phase relations. European Journal of Mineralogy, 12, 999–1014.
Sacerdoti, M., Passaglia, E., and Carnevali, R. (1995) Structure refinements of Na-, K-, and Ca-exchanged gmelinites. Zeolites, 15, 276–281.
Seki, Y., Onuki, H., Okumura, K., and Takashima, I. (1969) Zeolite distribution in the Katayama geothermal area, Onikobe, Japan. Recent Progress of Natural Sciences in Japan, 40, 63–79.
Shim, S.H., Navrotsky, A., Gaffney, T.R., and MacDougall, J.E. (1999) Chabazite: Energetics of hydration, enthalpy of formation, and effect of cations on stability. American Mineralogist, 84, 1870–1882.
Takaishi, T. (1998) Ordered distribution of Al atoms in the framework of analcimes. Journal of the Chemical Society-Faraday Transactions, 94, 1507–1518.
Takaishi, T. and Kato, M. (1995) Determination of the ordered distribution of aluminum atoms in zeolitic frameworks. Zeolites, 15, 689–700.
Takeuchi, Y., Mazzi, F., Haga, N., and Galli, E. (1979) Crystal structure of wairakite. American Mineralogist, 64, 993–1001.
Tchernev, D.I. (2001) Natural Zeolites in solar energy heating, cooling, and energy storage. In D.L. Bish and D.W. Ming, Eds. Natural Zeolites: Occurence, Properties, Applications, p. 589–617. Reviews in Mineralogy and Geochemistry, Mineralogical Society of America and the Geochemical Society, Washington, D.C.
Thompson, A.B. (1971) Analcite-albite equilibria at low temperatures. American Journal of Science, 271, 79–92.
Thrush, K.A. and Kuznicki, S.M. (1991) Characterization of chabazite and chabazite-like zeolites of unusual composition. Journal of the Chemical Society-Faraday Transactions, 87, 1031–1035.
Tingle, T.N., Neuhoff, P.S., Ostergren, J.D., Jones, R.E., and Donovan, J.J. (1996) The effect of "missing" (unanalyzed) oxygen on quantitative electron probe microanalysis of hydrous silicate and oxide minerals. Geological Society of America Abstracts with Programs, 28, 212.
Vega, A.J. (1983) A statistical approach to the interpretation of ^{29}Si NMR of zeolites. Acs Symposium Series, 218, 217–230.
Vezzalini, G., Quartieri, S., and Passaglia, E. (1990) Crystal structure of K-rich gmelinite and comparison with other refined gmelinite samples. Neues Jahrbuch für Mineralogie Monatshefte, 1990, 504–516.
Vezzalini, G., Quartieri, S., and Galli, E. (1997) Occurrence and crystal structure of a Ca-pure willhendersonite. Zeolites, 19, 75–79.
Wilkin, R.T. and Barnes, H.L. (1998) Solubility and stability of zeolites in aqueous solution: I. Analcime, Na-, and K-clinoptilolite. American Mineralogist, 83, 746–761.

Brought to you by | New York University Bobst Library Technical Services
Authenticated
Download Date | 1/21/16 12:53 PM

Wilkinson, J.F.G. and Hansel, H.D. (1994) Nephelines and analcimes in some alkaline igneous rocks. Contributions to Mineralogy and Petrology, 118, 79–91.

Woodcock, D.A., Lightfoot, P., Villaescusa, L.A., Diaz-Cabanas, M.J., Camblor, M.A., and Engberg, D. (1999) Negative thermal expansion in the siliceous zeolites chabazite and ITQ-4: A neutron powder diffraction study. Chemistry of Materials, 11, 2508–2514.

Xu, H.W., Navrotsky, A., Balmer, M.L., Su, Y.L., and Bitten, E.R. (2001) Energetics of substituted pollucites along the $CsAlSi_2O_6$-$CsTiSi_2O_{6.5}$ join: A high-temperature calorimetric study. Journal of the American Ceramic Society, 84, 555–560.

Yokomori, Y. and Idaka, S. (1998) The crystal structure of analcime. Microporous and Mesoporous Materials, 21, 365–370.

Zhao, P., Neuhoff, P.S., and Stebbins, J.F. (2001) Comparison of FAM mixing to single-pulse mixing in ^{17}O 3Q- and 5Q-MAS NMR of oxygen sites in zeolites. Chemical Physics Letters, 344, 325–332.

MANUSCRIPT RECEIVED JULY 25, 2002
MANUSCRIPT ACCEPTED SEPTEMBER 16, 2002
MANUSCRIPT HANDLED BY MICHAEL FECHTELKORD

Brought to you by | New York University Bobst Library Technical Services
Authenticated
Download Date | 1/21/16 12:53 PM